

pubs.acs.org/JPCB Article

# **Electrophoretic Mobility of Nanoparticles in Water**

Published as part of The Journal of Physical Chemistry B virtual special issue "Gregory A. Voth Festschrift". Dmitry V. Matyushov\*



Cite This: https://doi.org/10.1021/acs.jpcb.3c08172



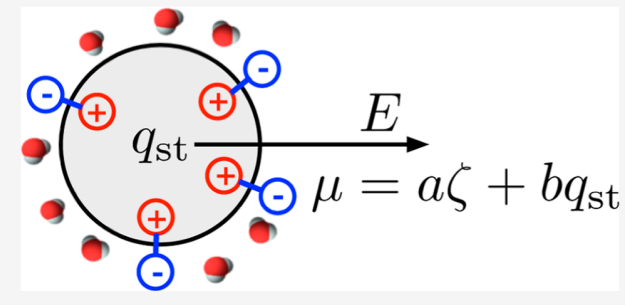
**ACCESS** 

III Metrics & More

Article Recommendations

Supporting Information

ABSTRACT: Classical equations for colloidal mobility anticipate linear proportionality between the nanoparticle mobility and zeta potential caused by the combined electrostatics of free charges at the nanoparticle and screening bound charges of the polar solvent. Polarization of the interfacial liquid, either spontaneous due to molecular asymmetry of the solvent (water) or induced by nonelectrostatic (e.g., charge-transfer) interactions, is responsible for a static interface charge adding to the overall electrokinetic charge of the nanoparticle. The particle mobility gains a constant offset term that is formally unrelated to the zeta potential. The static charge is multiplied by the static dielectric constant of the solvent in the expression for the electrokinetic charge and is



sufficiently large in magnitude to cause electrophoretic mobility of even neutral particles. At a larger scale, nonlinear electrophoresis linked to the interface quadrupole moment can potentially contribute a sufficiently negative charge to a micrometer-size nanoparticle.

#### **■ INTRODUCTION**

Electrophoretic mobility<sup>1,2</sup> is viewed as arising from the electrostatic force moving a charged nanoparticle in solution when placed in the uniform Maxwell electric field *E.* Standard theories use the following force equation as the basis for establishing the force balance to allow a constant-velocity drift

$$F_{\mathbf{q}} = q_{\mathbf{e}} E \tag{1}$$

The Maxwell field  $E = E^{\text{ext}} + E^{\text{b}}$  is a sum of the field of free external charges  $E^{\text{ext}}$  and the field of induced bound (molecular) charges  $E^{\text{b}}$  in the dielectric medium.<sup>3</sup>

The electrokinetic charge  $q_e$  in eq 1

$$q_e = q + q_{el} + q_{int} \tag{2}$$

combines the total charge of free carriers q at the particle with the total average charge of electrolyte ions  $q_{\rm el}$  within the surface of shear (stagnant layer)<sup>1,4</sup> dragged by the particle as it drifts through the liquid. The electrokinetic charge also contains an interface bound charge,  $q_{\rm int}$  including induced and stationary components (see below). The density of bound charge

$$\rho_{\rm int} = -\nabla \cdot \mathbf{P} \tag{3}$$

arises from the divergent character of the vector polarization field **P** in the interface.<sup>3,5</sup> Correspondingly, the interface charge  $q_{\text{int}}$  in eq 2 is the volume integral of the charge density  $\rho_{\text{int}}$ 

$$q_{\rm int} = \sigma S_{\rm R} \tag{4}$$

with  $S_{\rm R}=4\pi R^2$  specifying the surface area of the spherical dielectric cavity excluded from the surrounding liquid by the solute with its stagnant layer (radius R, Figure 1). The surface charge density<sup>3,5</sup>

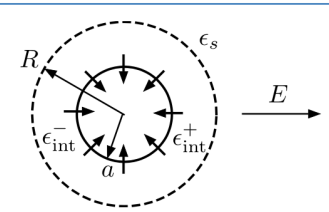


Figure 1. Spherical nanoparticle with the radius a and the concentric shear surface with the radius R. The bulk liquid carries the dielectric constant  $\epsilon_{\rm s}$  and the surface layer is assigned the dielectric constant  $\epsilon_{\rm th}^{\pm}$  characterizing the radial polar response perpendicular to the particle's surface, where + and — specify the response to outgoing and incoming fields, respectively. The arrows at the particle surface indicate preferentially oriented liquid dipoles creating polarization divergence and the corresponding surface charge density  $\sigma = P_{\rm n}$ . The polarization field shown in the diagram corresponds to  $\sigma > 0$ .

Received: December 14, 2023 Revised: February 27, 2024 Accepted: February 28, 2024

$$\sigma = P_{\mathbf{n}} = \hat{\mathbf{n}} \cdot \mathbf{P} \tag{5}$$

in eq 4 is the projection of the polarization field on the unit vector  $\hat{\mathbf{n}}$  pointing outward from the dielectric.<sup>5</sup> The surface charge  $q_{\text{int}}$  can be alternatively obtained from molecular simulations<sup>6–9</sup> by summing up molecular charges within the interfacial layer.

Dielectric theories view the bound charge as arising from liquid dipoles oriented along the field of the solute (Figure 1). Dipolar orientations induced by the electric field lead to the induced bound charge,  $q_{\rm b}$  responsible for dielectric screening. When only this induced part of the interface charge  $q_{\rm int}$  is included, one gets  $q_{\rm b} = -q(1-\epsilon_{\rm s}^{-1})$  for a spherical solute in the dielectric with the dielectric constant  $\epsilon_{\rm s}$ . The total charge associated with the ion,  $q+q_{\rm b}=q/\epsilon_{\rm s}$  becomes dielectrically screened.

The view of the induced character of the interfacial bound charge becomes incomplete when preferential orientations of interfacial liquid molecules are driven by interactions distinct from the electrostatic forces produced by the solute. In the standard view, there is no polarization when there are no electrical charges inducing it. In contrast, a divergent polarization field in eq 3 can be induced by specific 10 (e.g., chargetransfer solute-solvent interactions or arise spontaneously in the interface due to solvent's molecular asymmetry 12-15 as reflected by the temperature derivative of surface tension 16 and asymmetric surface wetting and electrostriction depending on the field direction. For instance, interfacial polarization spontaneously arises from the competition between dipolar and quadrupolar interactions to minimize the interface free energy. 15,16 For water, this spontaneous polarization results in a positive electrostatic potential inside of hard-sphere (HS) or Lennard-Jones (LJ) voids. 18-20 Electrostatic potential requires an electrostatic charge. This charge comes from the interfacial polarization unrelated to polarization induced by free charges adding a stationary component  $q_{st}$  to the overall interface charge in eq 2

$$q_{\rm int} = q_{\rm b} + q_{\rm st} \tag{6}$$

The main question explored here is the effect of  $q_{\rm st} \neq 0$  on the electrophoretic mobility.

The free and counterion charges are often combined,  $q+q_{\rm el}=qf(\kappa R)$ , through Henry's function depending on the inverse Debye—Hückel length  $\kappa=\Lambda^{-1}$  and the radius of the spherical shear surface R. This function bridges two limiting solutions of the Navier—Stokes equation for the drift of a spherical ion in an incompressible liquid: Smoluchowski's limit,  $f(\kappa R) \simeq 1$ ,  $\kappa R \gg 1$ , and Hückel's limit,  $f(\kappa R) \simeq 2/3$ ,  $\kappa R \ll 1$ .

The general solution for electrophoretic mobility  $\mu$ , given as the ratio of the drift velocity to the uniform Maxwell field, reads (Gaussian units<sup>3</sup>)

$$\mu = \frac{\epsilon_{\rm s} \zeta}{4\pi \eta} f(\kappa R) \propto \zeta \tag{7}$$

where  $\eta$  is the liquid shear viscosity and  $\varepsilon_s$  is the bulk dielectric constant connecting the uniform field of external charges to the Maxwell field:  $E=E^{\rm ext}/\varepsilon_s$ . Note that  $4\pi$  in the denominator in eq 7 is replaced with the inverse vacuum permittivity  $\varepsilon_0^{-1}$  in SI units.<sup>3</sup>

Equation 7 is derived by including free, q, electrolyte,  $q_{\rm el}$ , and induced bound,  $q_{\rm b}$ , charges in eq 2. This assumption allows one to express mobility in terms of the  $\zeta$  potential  $^{1,2,2,2}$   $\zeta = (q+q_{\rm el}+q_{\rm b})/R$  equal to the electrostatic potential at the shear surface

arising from free and induced bound charges. Here, we want to include the static interface charge  $q_{\rm st}$  and, in addition, lift the assumption of liquid incompressibility used in the Navier–Stokes equation employed in deriving the Helmholtz–Smoluchowski equation (see the Supporting Information). To achieve this goal, the problem is somewhat simplified by turning to Hückel's limit when mobility can be derived from a simple force balance condition assuming  $\kappa R \ll 1$ . One can neglect the effect of the electrolyte atmosphere in the limit of a low electrolyte concentration<sup>22,23</sup>  $c \simeq 10^{-5}$  M, when  $\Lambda \simeq 0.3/\sqrt{c}$  nm in water (c is in M) becomes equal to  $10^2$  nm. Given that screening by the electrolyte can be negligible under these conditions, the focus of the theory is on the electrostatic force acting on a nanoparticle in a compressible polar liquid.

The main goal of this article is to explore the limitations of the main result of the classical theory predicting  $\mu \propto \zeta$  (eq 7). This standard framework has been challenged by computer simulations on an umber of recent measurements employing nonlinear sum-frequency scattering techniques. The latter give access to both the alteration of the hydrogen-bond structure in the interface and, more importantly, to the interfacial electrostatics (see ref 27 for a recent review). It was shown that mobility can be significantly altered, by changing the solution pH, without affecting the measured  $\zeta$  potential.

Direct proportionality,  $\mu \propto \zeta$ , between mobility and  $\zeta$  potential is replaced here by a linear dependence, with an offset, when the stationary component of the interfacial charge  $q_{\rm st}$  is allowed in eq 6. The derivation presented below accounts not only for this new part of the interfacial charge but also for a reduced dielectric constant in the interface,  $^{1,28}$   $e_{\rm int} \ll e_{\rm s}$ . Equating the electrostatic force acting on the nanoparticle as derived below to the hydrodynamic friction force  $F_{\rm hydr} = 6\pi\eta uR$  (u is the drift velocity) in Hückel's limit,  $^{21}$  one obtains the following equation for the electrophoretic mobility (f=2/3 in eq 7)

$$\mu = \frac{\gamma \epsilon_s \zeta}{6\pi \eta} + \frac{q_{st} \epsilon_s}{6\pi \eta R} \tag{8}$$

Here,  $\gamma \simeq 4/3$ , which does not appear in the standard derivations for incompressible liquids, <sup>1,21</sup> is a correction factor due to the medium compressibility affecting the bulk dielectric constant. Furthermore, the  $\zeta$  potential in eq 8 is defined with the account for the local interfacial dielectric constant as produced by the combined effect of free and induced bound charges

$$\zeta = \frac{q + q_{\rm b}}{R} = \frac{q}{\epsilon_{\rm int}R} \tag{9}$$

It is important to stress that the appearance of dielectric constants  $\epsilon_s$  and  $\epsilon_{\rm int}$  in eqs 8 and 9 is the consequence of recognizing the bound charge as a part of the overall electrokinetic charge interacting with the external field. This logic dictates the inclusion of the charge  $q_{\rm st}$  in the same general formulation, leading to the second term in eq 8. Its appearance is what primarily distinguishes the present formulation from the standard framework of colloid science. One can bring eq 8 to the standard form in eq 7 by defining the stationary component of the  $\zeta$  potential

$$\zeta_{\rm st} = \frac{q_{\rm st}}{R} \tag{10}$$

Equation 8 is turned back to Hückel's limit (f=2/3 in eq 7) by extending the definition of  $\zeta$  potential to include the stationary charge component:  $\zeta \to \zeta + \zeta_{\rm st}$ . Note that, in contrast to the ordinary  $\zeta$  potential,  $\zeta_{\rm st}$  in eq 10 does not involve dielectric screening since self-screening of bound charges is not a part of standard theories of polar response. We also note that the standard derivation of Smoluchowski's limit<sup>1,21</sup> applies when the definition of  $\zeta$  potential is extended to include the stationary component  $\zeta_{\rm st}$  (Supporting Information).

Even though there are advantages in restoring the standard eq 7 by redefining the meaning of the  $\zeta$  potential to include the stationary charge, one has to keep in mind that standard approaches to manipulate the magnitude of  $\zeta$  through changing the electrolyte concentration and pH will apply only to its traditional form defined by eq 9. The stationary potential in eq 10 is determined by the interfacial liquid structure and is little affected by such manipulations as long as the concentrations of solution ions stay low, and strong specific adsorption altering the interfacial structure does not occur.

## ■ INDUCED AND STATIONARY INTERFACE CHARGE

An ensemble of polarized dipoles at the particle's surface is responsible for the surface charge density  $\sigma$  (eq 5) as long as the normal projection of the polarization field is nonzero (Figure 1). As mentioned above (eq 6), it includes two components. The induced bound charge  $q_b$  quantifies polarization in the direction perpendicular to the particle surface. This polar response is characterized by the longitudinal dielectric susceptibility of the interface. <sup>29</sup> If the bulk dielectric constant  $\epsilon_s$  is used for the longitudinal response, one obtains  $q_b = \sigma_b S_R = -q(1-\epsilon_s^{-1})$ . This charge creates the electrostatic potential  $\phi_b = q_b/r$ , which combines with the potential of free charges  $\phi_0 = q/r$  in the dielectrically screened potential  $\phi = q/(\epsilon_s r)$ . The induced bound charge  $q_b$  is thus a real physical charge responsible for dielectric screening. <sup>30</sup> The electrostatic force acting on the particle is modified by  $q_b$ .

There are significant reasons to question this outcome of standard dielectric theories. A number of recent computational<sup>6,31-33</sup> and experimental<sup>28,34</sup> studies have reinforced the decades-long conjecture 1,35,36 that the longitudinal dielectric response is substantially altered in the interface compared to the bulk and needs to be characterized by the interface dielectric constant  $\epsilon_{\rm int}$  which represents the capacitance of a thin film of water at the surface of a planar substrate or a spherical solute. This term is somewhat misleading ("susceptibility" would be a better option  $^{29}$ ) since  $\epsilon_{\mathrm{int}}$  is not a material constant and depends on both the substrate and the field strength (see below). The new evidence, which also dispels the long-standing assumption that the reduction of the dielectric response has to deal with a strong field of the substrate, 37,38 assigns a lower dielectric constant to an interfacial layer with the thickness of  $\delta \simeq 1$  nm. Its exact magnitude depends on the local structure and substrate, but all calculations indicate  $\epsilon_{\rm int} \ll \epsilon_{\rm s}$ . The same picture applies to the radial polar response at the surface of a spherical solute<sup>29</sup> applicable to nanoparticle mobility.

By construction of being induced by an external field,  $^{3,5,39}$  dielectric response, even when modified by adopting an interface dielectric constant, does not anticipate an interfacial polarization in the absence of the polarizing field of free charges. This is not true for liquids carrying both molecular dipoles and molecular quadrupoles,  $^{12,15}$  where spontaneous interfacial polarization arises from the competition between molecular multipoles.  $^{18-20}$  It leads to a nonzero surface charge density  $\sigma_{\rm st}$  and the

corresponding charge  $q_{\rm st}$  (eq 6) connected by surface integration

$$q_{\rm st} = \oint \mathrm{d}S \sigma_{\rm st} \tag{11}$$

This charge is not related by a linear response function to the external field and, thus, does not appear in linear-response theories. The breaking of symmetry  $q_{\rm st} = 0$  at E = 0 is caused by an intrinsic interfacial structure or by strong solute—solvent interactions not reducible to solute—solvent electrostatics.

The surface charge is nonzero even for uncharged solutes. Indeed, simulations of neutral solutes interacting with water by Kihara potential<sup>40</sup> (hard-sphere repulsion with surface LJ potential) produced  $\sigma_{\rm st} \simeq 0.01 \; {\rm e/nm^2}$ . A similar magnitude,  $\sigma_{\rm st}$  $\simeq -0.016$  e/nm<sup>2</sup>, was found in quantum density-functional calculations of the oil-water interface. In the latter case, the charge arises from charge-transfer interactions between water and oil molecules, leading to transfer of partial electronic density to oil and thus creating a set of interfacial dipoles oriented oppositely to those shown in Figure 1 and responsible for a negative surface charge. Also recent density-functional molecular dynamics simulations of water on graphene and boronnitride substrates<sup>41</sup> uncovered an overall ferroelectric order of interfacial water arising from locally antiparallel alignments of water dipoles. The overall alignment is toward the bulk yielding  $\sigma_{\rm st} = -0.36 \text{ e/nm}^2$ . The sign of the surface charge density is consistent with that of the oil-water interface, and the magnitude is sufficiently large to make connection to mobility measurements.42

Despite the discrepancy between fixed-charge and delocalized-charge calculations, an important observation here is that a negative electrokinetic charge of neutral particles is not an intrinsic property of the water-hydrophobic interface but, on the contrary, is a strong function of specifics of the solute—water interactions. Orientations of interfacial waters are affected by interactions with the substrate 7,43,44 and by water force fields in numerical simulations. 41,45 The bound surface charge was found to scale linearly with the size of the Kihara solute in MD simulations,  $q_{\rm st} \propto R$ , yielding a constant potential,  $\zeta_{\rm st} \simeq 300~{\rm mV}$  for nanometer-size particles<sup>20,40</sup> (Figure 2). The stationary potential  $\zeta_{\rm st}$  associated with the integrated surface charge density (eq 11) is identical to the average potential produced by water surrounding a neutral solute ( $\phi_s(0)$ , Figure 3a). These positive potentials are sufficiently large in the magnitude but are of opposite sign to  $\zeta \simeq -70 \text{ mV}$  at pH = 7 obtained for  $\simeq 50 \,\mu\text{m}$  air bubbles in distilled water<sup>22</sup> or  $\zeta \simeq -100$  mV for hexadecane

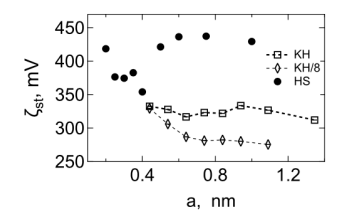


Figure 2. Static component of the  $\zeta$  potential (eq 10) at the surface of charge-neutral hard-sphere (HS) and LJ (modeled with the Kihara (KH) potential) solutes with varying radius a. Points are average electrostatic potentials produced by water at geometric centers of neutral solutes from MD simulations in TIP3P water at 298 K. Two sets of LJ solutes use different values of the solute—solvent LJ energy: 3.7 (KH) and 8.0 (KH/8) kJ/mol. Adapted with permission from Figure S1 in ref 40 Copyright 2015 American Institute of Physics.

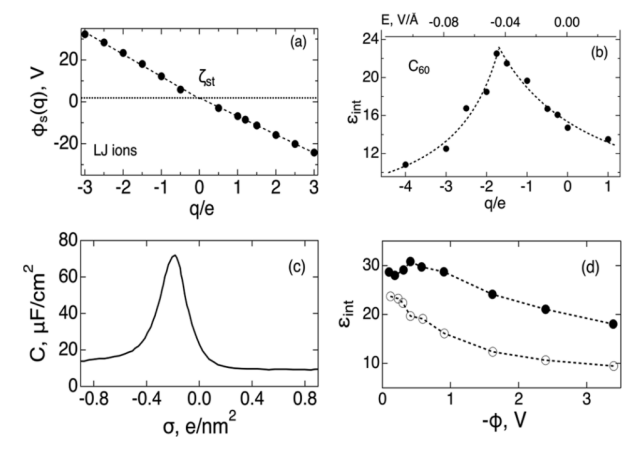


Figure 3. (a) Electrostatic potential  $φ_s(q)$  of polarized SPC/E water at the centers of LJ ions with constant radius and altering charge:  $ζ_{st}$  marks  $φ_s(0)$ . Reproduced from ref 48 Copyright 2022 American Physical Society. (b) Dependence of the interface dielectric constant of SPC/E water on the charge of C<sub>60</sub> fullerenes and the electric field acting on oxygens of water closest to C<sub>60</sub>. Adapted from ref 49 Copyright 2019 American Chemical Society. (c) Capacitance of an aqueous NaF–Ag(100) interface vs the surface charge density of the electrode. Reproduced from ref 50 Copyright 2023 American Physical Society. (d) Dielectric constant of ≃8 Å water layer at the graphene sheets of a plane capacitor vs the capacitor potential. Points refer to outgoing (open) and incoming (filled) fields. Reproduced from ref 9 Copyright 2023 American Physical Society.

drops in pH = 7, 0.4 mM electrolyte. Which smaller values,  $\simeq$ -10 mV were reported for hexadecane nanodrops at pH = 7 when stringent cleaning was implemented to eliminate surface contaminants. The Furthermore, addition of anionic surfactants flipped interfacial water molecules to inward orientations, as shown in Figure 1. The resulting  $\zeta \simeq -50$  mV arises as a compensation between a negative q and positive  $q_{st}$  in eqs 2 and 6. Assuming that  $\zeta \simeq -10$  mV is caused by water dipoles pointing to the bulk, one can anticipate an orientational structural crossover with an increased density of anionic surfactants (see below).

The prediction of a nonzero interface bound charge at q = 0extends to ion solvation. Simulations of ions in force-field water  $^{48,51-53}$  have shown that the electrostatic potential  $\phi_{\rm s}(q)$  of the polarized liquid at the center of the polarizing charge is linear in q for both cations and anions (Figure 3a). However, the magnitude of the slope of  $\phi_s(q)$  vs q is higher for anions than that for cations. Moreover, both branches of  $\phi_s(q)$  vs q extrapolate to a nonzero value  $\phi_s(0) = \zeta_{st}$  at q = 0. For instance,  $\zeta_{st} \simeq 1.94 \, \text{V}$ , as shown in Figure 3a, was found for a number of cations and anions in SPC/E water with the same radius  $a \simeq 3.6$  Å and varying  $q_s^{48}$  This value implies  $\sigma_{\rm st} \simeq 0.3 \ {\rm e/nm^2}$ , significantly exceeding the charge density  $\sigma_{\rm st} \simeq 0.01 \ {\rm e/nm^2}$  around hardsphere and LJ solutes. The reason is a strongly collapsed hydration shell around small ions compared to larger hardsphere and LJ solutes (Figure 2). One can anticipate that adsorption of impurities and solution ions can result in higher local values of  $\sigma_{\rm st}$  and higher integrated bound charges  $q_{\rm st}$  (eq 11) of hydrated nanoparticles.

Different slopes of  $\phi_s(q)$  vs q for cations and anions also indicate that different values of the interface dielectric constant need to be assigned to incoming (anions) and outgoing (cations) electric fields if the standard dielectric framework is adopted to describe the void potential. This result must be

anticipated given the asymmetry of water's molecular charge and the resulting nonaxial molecular quadrupole. <sup>54</sup> Aligning water molecules along the outgoing electric field puts water's hydrogens into the bulk, while formation of dangling O–H bonds <sup>55</sup> is required to orient water molecules along an incoming electric field. Based on these considerations, one has to assume

$$\epsilon_{\rm int}^+ < \epsilon_{\rm int}^-$$
 (12)

where + and - are assigned to the outgoing (cations, q > 0) and incoming (anions, q < 0) fields, respectively (Figure 1).

Equation 12 implies asymmetry of the interfacial dielectric response upon the change in the direction of the field normal to the surface.<sup>17</sup> Such a dependence on the field direction is realized experimentally by altering the sign of the substrate charge. A number of recent studies, both computational<sup>9,50,56</sup> and experimental,<sup>57–61</sup> have pointed to the dependence of interfacial structure on the substrate charge (see ref 43 for a recent review). The dependence of dynamics on the substrate charge is more controversial.<sup>62,63</sup>

Asymmetric and nonlinear dielectric response of  $D_2O$  interfacing graphene was reported from sum-frequency generation spectroscopy,  $^{61}$  but the analysis of data was recently challenged. The onset of the nonlinear/anisotropic dielectric response was assigned to the release of dangling OD bonds at the surface electric field of  $E^{\rm ext} \simeq 0.04 \, {\rm V/\AA}.^{61} \, {\rm A}$  similar transition, at the field of  $\simeq 0.046 \, {\rm V/Å}$ , was found in simulations of SPC/E water at the surface of  $C_{60}$  fullerenes  $^{49}$  with varying solute charge (Figure 3b). The existence of structural interface crossovers releasing dangling OH bonds was supported by in situ surface-enhanced Raman  $^{60}$  and X-ray absorption  $^{58}$  spectroscopies.

The interface dielectric constant passes through a spike as a function of fulleren's charge or the electric field acting on the surface waters (Figure 3b). This result implies that  $\epsilon_{\rm int}(E^{\rm ext})$  depends on both the orientation and the strength of the external field, making the interfacial polarization response nonlinear. Both conclusions were confirmed by simulations of water in a slab between two graphene sheets (Figure 3d). Note that  $\epsilon_{\rm int}$  is calculated in Figure 3b as a linear response to a small field perturbation. This procedure corresponds to experiments in which as small AC bias is added to a large DC bias to determine  $\epsilon(E)$  of a bulk material.

The existence of a maximum of the interface dielectric constant at a negative surface charge density implies a corresponding maximum of capacitance  $C \propto \epsilon_{\rm int}(\sigma)$  (Figure 3c). A spike in capacitance at a negative electrode potential (relative to the potential of zero charge) was indeed observed in impedance measurements. Simulations  $^{50,56}$  show that the sign of the electrode potential at the capacitance maximum is specified by molecular properties of the solvent, and it switches from negative to positive when water is replaced with acetonitrile.  $^{50}$ 

To summarize, there is substantial body of evidence in support of anisotropy of the interface dielectric constant, as indicated by eq 12. This result is used below to present a plausible model for the quadrupolar moment of the interface polarized by an external field. Estimates based on dielectric anisotropy, as shown in Figure 3, indicate that this term in the effective electrokinetic charge might dominate the mobility of micrometer-size nanoparticles. There is currently no established protocol to directly measure  $\epsilon_{\text{int}}^{\pm}$  and one has to rely on simulations such as those shown in Figure 3d. In the context of the formal theory presented below,  $\epsilon_{\text{int}}^{\pm}$  is viewed as a theory parameter to be determined independently.

## **■ ELECTROSTATIC FORCE**

The electrostatic force acting on a particle in the liquid involves two components:  $^{67}$  (1) the volume force produced by mechanical deformation of the interface caused by the field and (2) the force of the interaction of the external field  $E^{\rm ext}$  with the total density of charge  $\rho_{\rm F}$ . Directing the external field along the z-axis of the laboratory frame sets up axial symmetry for the problem adopted in our calculations. The total electrostatic force  $F_z$  acting on the nanoparticle is a sum of the volume force  $f_z$  and the interaction with the external field

$$F_z = f_z + \int \mathrm{d}\mathbf{r} \rho_t E^{\text{ext}} \tag{13}$$

This expression involves the total charge density  $\rho_t = \rho_0 + \rho_b + \rho_{\rm st}$  combining the solute charge density,  $\rho_0$ , with the induced,  $\rho_{\rm b}$ , and stationary,  $\rho_{\rm sv}$  densities of the interface. Standard electrostatic arguments <sup>67</sup> lead to an expression for the dielectric volume force in terms of the spatial, stress-induced, alteration of the dielectric constant and its change due to isothermal compression altering the density  $\rho$ 

$$f_{\alpha} = -\frac{E^2}{8\pi} \partial_{\alpha} \epsilon_{\rm s} + \partial_{\alpha} \left( \frac{E^2}{8\pi} \rho \left( \frac{\partial \epsilon_{\rm s}}{\partial \rho} \right)_{\rm T} \right)$$
(14)

The two terms in eq 13 can be combined by noting that  $4\pi(\rho_0 + \rho_b) = \partial_\alpha E_\alpha$  (Gaussian units), where summation over common Cartesian indexes  $\alpha = x$ , y, and z is assumed. After standard transformations <sup>67,68</sup> (see the Supporting Information for full derivation), one arrives at a sum of the interaction of the static charge with the field of external charges and a surface integral of the Maxwell stress tensor  $^3$   $T_{z\alpha}$  over the spherical shear surface

$$F_z = q_{\rm st} \epsilon_{\rm s} E + \oint T_{z\alpha} \hat{n}_{\alpha} dS \tag{15}$$

The stress tensor in this expression is contracted with the components  $\hat{n}_{\alpha}$  of the surface vector **n** normal to the shear surface and pointing outward from the dielectric medium<sup>5</sup> (toward the particle's center in the present case). The integral is taken over the shear surface with radius R, which is assumed to be identical with the particle surface given that  $|R - a| \ll R$  for most practical situations (Figure 1).

The material Maxwell stress tensor<sup>3,5,67</sup> in eq 15 is a sum of the second-rank tensor component

$$\sigma_{\alpha\beta} = \frac{\epsilon_{\rm s}}{4\pi} \left[ E_{\alpha} E_{\beta} - \frac{1}{2} \delta_{\alpha\beta} E^2 \right] \tag{16}$$

and a diagonal contribution arising from isothermal compression as expressed by the second term in the following equation

$$T_{\alpha\beta} = \sigma_{\alpha\beta} + \frac{1}{8\pi} \delta_{\alpha\beta} E^2 \rho \left( \frac{\partial c_s}{\partial \rho} \right)_{T}$$
(17)

The only distinction of eq 15 from the standard dielectric theories is the appearance of the interaction term between the stationary interface charge and the applied field;  $q_{\rm st}=0$  is assumed in the dielectric theories.

With axial symmetry (Figure 1), only two projections of the field at the shearing surface matter for the calculation: radial,  $E_{\rm r} = -\partial\phi/\partial r$ , and tangential,  $E_{\rm t} = -(1/r)\partial\phi/\partial\theta$ . The first term in the stress tensor [eqs 16 and 17] produces the following z-projection of the force<sup>69</sup>

$$F_z^{(1)} = \frac{\epsilon_s R^2}{4} \int_{-1}^{1} [(E_r^2 - E_t^2) \cos \theta - 2E_r E_t \sin \theta] d\cos \theta$$
 (18)

where  $\theta$  is the polar angle relative to the z-axis. Correspondingly, the second term in eq 17 yields

$$F_z^{(2)} = \frac{R^2}{4} \rho \left(\frac{\partial \epsilon_s}{\partial \rho}\right)_{\rm T} \int_{-1}^1 (E_{\rm r}^2 + E_{\rm t}^2) \cos\theta \, d\cos\theta \tag{19}$$

The radial and tangential field projections in eqs 18 and 19 are defined as the corresponding derivatives of electrostatic potential  $\phi(\mathbf{r})$  evaluated at the shear surface. The electrostatic potential is in turn produced by the external field, free charges of the solute, and induced bound charges in the interface. The latter two can be combined in the surface charge density  $\sigma(\theta)$  expanded,  $^{70}$  due to axial symmetry, in Legendre polynomials  $P(\cos\theta)$ 

$$\sigma(\theta) = \sum_{l=0}^{\infty} \sigma_l P_l(\cos \theta)$$
(20)

To reduce the problem to well-defined multipolar moments, only the first three expansion terms in eq 20 are included. The zero-order term  $S_{\rm R}\sigma_0=q+q_{\rm b}$  combines the ionic solute charge with the bound charge induced at the interface. Assuming that the longitudinal interface response is specified by the interface dielectric constant  $^{6,31-33}$   $\epsilon_{\rm inv}$  one obtains  $S_{\rm R}\sigma_0=q/\epsilon_{\rm int}$  (see the Supporting Information). Note that the inhomogeneous Maxwell field in our formalism is caused by charge densities  $\rho_0$  and  $\rho_{\rm b}$ . Equal results are obtained by including the charge density  $\rho_{\rm st}$  in the Maxwell equation for the field upon the corresponding changes to the zeroth projection of the surface charge density  $\sigma_0$ . This is not done in the present formulation since the Maxwell tensor in the medium involves the bulk dielectric constant defined only with respect to induced bound charges. The external force acting of  $q_{\rm st}$  is therefore considered separately in eq 15.

The l = 1, 2 expansion terms in (20) are induced by the applied field and are thus proportional to E. The first-order term is responsible for the interface dipole moment<sup>71</sup>

$$M_0^{\rm int} = \sigma_1 \Omega_0 \tag{21}$$

where  $\Omega_0=(4\pi/3)a^3$  is the particle volume. This parameter often appears in theories of dielectrics. Assigning the dielectric constants  $\epsilon_{\rm int}$  and  $\epsilon_0$  to the interface and solute, respectively, one obtains  $^{3,68}$ 

$$M_0^{\text{int}} = -a^3 \frac{\epsilon_{\text{int}} - \epsilon_0}{2\epsilon_{\text{int}} + \epsilon_0} E \tag{22}$$

The interface dipole interacts with the gradient of the external electric field to produce a dielectrophoretic force acting on large polarizable nanoparticles.<sup>72</sup> The second-order expansion term in eq 20 is responsible for the *zz*-projection of the second-rank quadrupole moment of the interface

$$Q_{zz}^{\text{int}} = \frac{3}{5}\sigma_2 a \Omega_0 \tag{23}$$

This interface multipole is also proportional to the external field and contributes a term linear in the field (nonlinear transport coefficient) to the mobility. Combining the field of external charges with the field of the free and induced bound charge, one obtains<sup>3</sup> the electrostatic potential at the point **r** such that  $r \ge R$ 

$$\phi(\mathbf{r}) = -Er\cos\theta + S_R \sum_{l=0}^{\infty} \frac{R^l}{r^{l+1}} \frac{(l+1)\sigma_l}{2l+1} P_l(\cos\theta)$$
(24)

By truncating the summation in eq 24 after the third term, one can use the radial and transverse field components in eqs 18 and 19 to obtain the total force acting on the particle

$$F_z = q_{\rm st} \epsilon_{\rm s} E + q_{\rm eff}^{(1)} E + q_{\rm eff}^{(2)} \frac{2M_0^{\rm int}}{3R^3}$$
 (25)

The effective charges  $q_{\text{eff}}^{(1)}$  and  $q_{\text{eff}}^{(2)}$  in this equation are

$$q_{\text{eff}}^{(1)} = \frac{q\epsilon_{\text{s}}}{\epsilon_{\text{int}}} \left( 1 + \frac{1}{3} \left( \frac{\partial \ln \epsilon_{\text{s}}}{\partial \ln \rho} \right)_{\text{T}} \right)$$
(26)

and

$$q_{\text{eff}}^{(2)} = \epsilon_{\text{s}} (\epsilon_{\text{int}}^{-1} q + q_{\text{Q}}) \left( \frac{\partial \ln \epsilon}{\partial \ln \rho} \right)_{\text{T}}$$
(27)

The charge associated with the interface quadrupole moment becomes

$$q_{Q} = \frac{9}{5R^2} Q_{zz}^{\text{int}} \tag{28}$$

Adopting the continuum estimate for the interface dipole moment (eq 22) and dropping the interface quadrupole moment for the nanometer-scale solutes (see the estimates below), two effective charges can be combined in one charge interacting with the external field. One arrives at eq 1 with the electrokinetic charge  $q_{\varepsilon}$  given by the following relation

$$q_{e} = q_{st} \epsilon_{s} + q \gamma (\epsilon_{s} / \epsilon_{int})$$
(29)

where the compression correction factor here and in eq 8 is

$$\gamma = 1 + \frac{\epsilon_0}{2\epsilon_{\rm int} + \epsilon_0} \left( \frac{\partial \ln \epsilon_{\rm s}}{\partial \ln \rho} \right)_{\rm T}$$
(30)

The second term in this equation involves the standard Onsager cavity screening factor  $^{39}$  multiplied with the logarithmic derivative of the dielectric constant over density. This term needs to be maintained since  $(\partial \ln \varepsilon_{\rm s}/\partial \ln \rho)_{\rm T} \simeq 1$  for many polar liquids and is equal to 1.04 for room-temperature water.  $^{68}$ 

The derivation thus far is very general. It adopts the material Maxwell stress tensor<sup>3,5,67</sup> eliminating the assumption of an incompressible interfacial liquid but does not make any specific assumptions about the microscopic interfacial structure. The main quantitative result is underscreening of the particle charge and a corresponding force enhancement by a factor of  $\epsilon_{\rm s}/\epsilon_{\rm int}$  in eq 29. Obviously, the force converts to the standard dielectric result,  $F_z = qE$ , when  $\epsilon_{int} = \epsilon_{st} \gamma = 1$ , and  $q_{st} = 0$ . The contribution of the quadrupolar interfacial moment to the effective interface charge is further enhanced if the tangential field is put equal to zero  $[E_t = 0 \text{ in eqs } 18 \text{ and } 19]$ , which assumes that surface charges do not sustain a tangential force allowing the liquid to flow in the shear surface. This boundary condition is not applied here, but even the present framework makes the interface quadrupolar moment significant for micrometer-scale particles (see below).

The surface charge of a nanoparticle associated with free carriers arises from electrolyte and hydroxide/hydronium ions, other impurities binding to the particle's surface, and from ionization of specific surface group (such as surface residues for proteins). In the present content, surface impurities contribute to  $\sigma_0$  and potentially modify  $\varepsilon_{\text{int}}^{\pm}$ . The mechanism of impurities affecting the  $\zeta$  potential still anticipates  $\mu \propto \zeta$  (eq 7), which was disputed by recent measurements.

An asymmetric distribution of bound charge should in principle produce higher moments  $\sigma_l$ , l > 0 of the surface charge density. However, all such charge asymmetries average out by particle rotations, leading to  $\sigma_0$  as the only term in eq 20 independent of the externally applied field. Terms with l > 0[dipole and quadrupole in eqs 21 and 23] are induced by the external field and thus scale as  $\propto E$  in the lowest order. The interface dipole (eq 21) is responsible for the reaction-field term multiplying the logarithmic density derivative of the dielectric constant in eq 30 and does not contribute to nonlinear mobility. On the contrary, the quadrupolar interface moment, also scaling linearly with the applied field, produces a force term quadratic in the field, thus leading to a nonlinear transport coefficient, 74 which, for polyelectrolytes, was attributed to field-induced deformation of the ionic cloud.<sup>75</sup> While different mechanisms can contribute to  $q_0$  in eqs 27 and 28, we evaluate it here by applying the direction-anisotropic interface dielectric constant  $\epsilon_{\text{int}}^{\pm}$  discussed above (eq 12 and Figure 3).

If the dielectric constants  $e_{\text{int}}^{\pm}$  corresponding to the outgoing (+) and incoming (-) fields (Figure 1) are assigned to two lobes of the spherical solute in Figure 1, one obtains (see the Supporting Information)

$$Q_{zz}^{\text{int}} = \frac{R^4}{16} E \left( \frac{1}{\epsilon_{\text{int}}^+} - \frac{1}{\epsilon_{\text{int}}^-} \right) > 0$$
 (31)

where the last inequality follows from eq 12. As anticipated,  $Q_{zz}^{int}$  scales linearly with E, resulting in a contribution to the force quadratic in the field (mobility linear in the field). At zero solute charge, q = 0, one obtains by adopting the interface dipole in eq 22.

$$q_{\rm e} = \epsilon_{\rm s} q_{\rm st} - \frac{3\epsilon_{\rm s} R^2}{40} E \left( \frac{1}{\epsilon_{\rm int}^+} - \frac{1}{\epsilon_{\rm int}^-} \right) \left( \frac{\partial \ln \epsilon_{\rm s}}{\partial \ln \rho} \right)_{\rm T}$$
(32)

A negative contribution to electrokinetic charge from induced interface quadrupole, consistent with mobility measurements of oil drops,  $^{22}$  scales as  $\propto R^2$ . One can estimate this term by adopting an experimentally accessible electric field of  $E \simeq 10^3 \, \text{V/}$ m and  $\epsilon_{\rm int}^+ = 10$ , and  $\epsilon_{\rm int}^- = 11$  (Figure 3b). One then obtains the surface charge density  $\simeq -26 \text{ e/nm}^2$  from the quadrupolar term for a  $R \simeq 1 \ \mu m$  particle with  $(\partial \ln \epsilon_s / \partial \ln \rho)_T = 1.04$  for water.<sup>68</sup> This estimate, which can be improved with  $\epsilon_{ ext{int}}^{\pm}$  from direct simulations, allows one to drop the interface quadrupole for a nanometer-scale particle (eq 29) but also shows a large negative effective charge for a micrometer-scale nanoparticle. The effective charge in the latter case is linked to anisotropy of water's interfacial dielectric response. 9,49,50 It is important to stress that this negative electrokinetic charge is allowed by solvent compressibility producing a nonzero  $(\partial \ln \epsilon_s / \partial \ln \rho)_T$  in eq 32. This term does not appear in standard theories, adopting an incompressible solvent in the Navier-Stokes equation.

## DISCUSSION

Mobility measurements of surfactant-free emulsions and air drops have consistently demonstrated their negative effective charges ( $\zeta < 0$ , eq 7). <sup>23,76</sup> Hydroxide adsorption <sup>77,78</sup> as the sole origin of this effect was questioned as it requires very large adsorption free energies <sup>79</sup> and contradicts to direct measurements of the concentration of hydroxide ions in the interface. <sup>80–82</sup> While the possibility of contamination by impurities has to be considered, <sup>47,73</sup> other mechanisms of producing the effective negative charge have been proposed. <sup>42</sup>

This article presents an analytical formalism for the electrostatic force acting on a nanoparticle based on the proposition 10,70,83 that polarization of the interface, unrelated to the polarizing field of free charges, produces an effective charge interacting with an external electric field to allow dragging force. The interface is still neutral, and the effective charge comes from the divergence of the vector polarization field (Figure 1). The charge from nonelectrostatic polarization  $q_{\rm st}$  comes in addition to the standard induced (bound) charge  $q_b$  responsible for dielectric screening and also arising from polarization divergence.<sup>30</sup> The charges  $q_{st}$  and  $q_b$  (eq 6) are related to the same physics of divergent interface polarization, but are assigned to, correspondingly, nonelectrostatic and electrostatic interactions with the solute. These charges contribute to the linear mobility, while the quadrupole effective charge  $q_0$  leads to the electrophoretic force quadratic in the applied field.

This universal mechanism for effective charging of both hydrophobic and hydrophilic interfaces makes the effective charge depend on the orientation of interfacial dipoles relative to the normal direction pointing inward from the solvent to the nanoparticle. It does not exclude zero charge of hydrophobic drops <sup>47</sup> if no preferential orientations of interfacial dipoles exist in the interface. However, since  $q_{st}\varepsilon_s$  enters the effective electrokinetic charge in eq 29, mobility is expected to be sensitive to the interfacial dipolar structure. In this view, the inward pointing dipoles, as shown in Figure 1, produce a positive charge found in numerical simulations of voids in fixed-charge force-field water models. <sup>18,19,40</sup> In contrast, recent ab initio simulations of oil—water and substrate—water interfaces have produced oppositely (outward) pointing interfacial dipoles accounting for the observed negative effective charge of nanoparticles.

The present model does not attempt to resolve the origin of the surface charge of the hydrophobic nanoparticles. Instead, it provides a theoretical framework within which this resolution can be sought. The key parameter of the theory, the interface stationary (noninduced) charge  $q_{\rm st}$  requires specific molecular mechanisms allowing the surface charge density arising from nonelectrostatic origin. The existing evidence points to surface charge densities sufficient for allowing the observed  $\zeta$  potential, at least at the size of nanometer particles. This notion is not new. Previous simulations of electrophoresis at the surface of a lipid bilayer found the electrostatic potential at the shear surface to exceed the electrokinetic potential by a factor of  $\simeq$ 25. The missing component was attributed to the "dipole potential" consistent with  $\zeta_{\rm st}$  in the present formulation.

It remains to be seen whether the present-day nanometerscale simulation evidence can be extended to submicrometer oil drops studied experimentally. What the present theoretical framework does not resolve is the specifics of the surface charge scaling with particle size. The plateau in  $\zeta_{st}$  potential with increasing size of a nanometer-scale particle shown in Figure 2 and observed in previous simulations<sup>18</sup> is puzzling. One would expect the density of surface-oriented dipoles to be constant and the stationary charge  $q_{\rm st}$  to scale linearly with the surface area<sup>46</sup> (also see eq 32), thus producing  $\zeta$  potential increasing linearly with the particle size. This is not what follows from the limited evidence produced by simulations so far. The reason might be sought in a compensating effect of the decreasing local density around larger solutes caused by weak dewetting of the hydrophobic—water interface at the nanometer scale <sup>40,84</sup> (particularly pronounced in a nonmonotonic  $\zeta_{\rm st}(a)$  for HS solutes in Figure 2).

The present estimates suggest that electrophoretic drift quadratic in the field can dominate for micrometer-sized nanoparticles because of a quadratic scaling of the corresponding charge  $q_Q \propto R^2$  with the particle size (eq 32). This outcome is experimentally testable as it predicts a linear scaling of mobility with the external field. A nonzero value  $\sigma_2 \neq 0$  of the second Legendre moment of water's interface charges is required to produce an interface quadrupole (eq 23). Its value was estimated here from anisotropy, in respect to the field direction, of the interface dielectric constant.  $^{9,49,50}$ 

### ASSOCIATED CONTENT

# Supporting Information

The Supporting Information is available free of charge at https://pubs.acs.org/doi/10.1021/acs.jpcb.3c08172.

Derivation of equations presented in the text (PDF)

# AUTHOR INFORMATION

## **Corresponding Author**

Dmitry V. Matyushov — School of Molecular Sciences and Department of Physics, Arizona State University, Tempe, Arizona 85287-1504, United States; ⊙ orcid.org/0000-0002-9352-764X; Email: dmitrym@asu.edu

Complete contact information is available at: https://pubs.acs.org/10.1021/acs.jpcb.3c08172

#### Notes

The author declares no competing financial interest.

#### ACKNOWLEDGMENTS

This research was supported by the National Science Foundation (CHE-2154465).

# REFERENCES

- (1) Hunter, R. J. Zeta Potential in Colloid Science; Academic Press: London, 1981.
- (2) Hunter, R. J. Foundations of Colloid Science, 2nd ed.; Oxford University Press: Oxford, 2001.
- (3) Jackson, J. D. Classical Electrodynamics, 2nd ed.; Wiley: New York, 1975.
- (4) Lyklema, J.; Rovillard, S.; De Coninck, J. Electrokinetics: The properties of the stagnant layer unraveled. *Langmuir* **1998**, *14*, 5659–5663.
- (5) Landau, L. D.; Lifshitz, E. M. Electrodynamics of Continuous Media; Pergamon: Oxford, 1984.
- (6) Bonthuis, D. J.; Gekle, S.; Netz, R. R. Dielectric profile of interfacial water and its effect on double-layer capacitance. *Phys. Rev. Lett.* **2011**, *107*, 166102.
- (7) Poli, E.; Jong, K. H.; Hassanali, A. Charge transfer as a ubiquitous mechanism in determining the negative charge at hydrophobic interfaces. *Nat. Commun.* **2020**, *11*, 901.

- (8) Dinpajooh, M.; Matyushov, D. V. Interface dielectric constant of water at the surface of a spherical solute. *J. Mol. Liq.* **2023**, 376, 121400.
- (9) Mulpuri, N.; Bratko, D. Polarity-dependence of the nonlinear dielectric response in interfacial water. *J. Chem. Phys.* **2023**, *158*, 134716.
- (10) Knecht, V.; Klasczyk, B.; Dimova, R. Macro- versus Microscopic View on the Electrokinetics of a Water—Membrane Interface. *Langmuir* **2013**, *29*, 7939—7948.
- (11) Pullanchery, S.; Kulik, S.; Rehl, B.; Hassanali, A.; Roke, S. Charge transfer across C—H—O hydrogen bonds stabilizes oil droplets in water. *Science* **2021**, *374*, 1366—1370.
- (12) Frenkel, J. Kinetic Theory of Liquids; Dover: New York, 1955.
- (13) Stillinger, F. H.; Ben-Naim, A. Liquid-vapor interface potential for water. J. Chem. Phys. 1967, 47, 4431–4437.
- (14) Luzar, A.; Svetina, S.; Žekš, B. Consideration of the spontaneous polarization of water at the solid/liquid interface. *J. Chem. Phys.* **1985**, 82, 5146–5154.
- (15) Horváth, L.; Beu, T.; Manghi, M.; Palmeri, J. The vapor-liquid interface potential of (multi)polar fluids and its influence on ion solvation. *J. Chem. Phys.* **2013**, *138*, 154702.
- (16) Croxton, C. A. Molecular orientation and interfacial properties of liquid water. *Phys. A* **1981**, *106*, 239–259.
- (17) Bratko, D.; Daub, C. D.; Leung, K.; Luzar, A. Effect of field direction on electrowetting in a nanopore. *J. Am. Chem. Soc.* **2007**, *129*, 2504–2510.
- (18) Ashbaugh, H. S. Convergence of molecular and macroscopic continuum descriptions of ion hydration. *J. Phys. Chem. B* **2000**, *104*, 7235–7238.
- (19) Beck, T. L. The influence of water interfacial potentials on ion hydration in bulk water and near interfaces. *Chem. Phys. Lett.* **2013**, 561–562, 1–13.
- (20) Matyushov, D. V. Electrostatic solvation and mobility in uniform and non-uniform electric fields: From simple ions to proteins. *Biomicrofluidics* **2019**, *13*, 064106–064116.
- (21) Ohshima, H. Theory of Colloid And Interfacial Electric Phenomena; Academic Press: London, 2006.
- (22) Takahashi, M. ζ-Potential of microbubbles in aqueous solutions: Electrical properties of the gas-water interface. *J. Phys. Chem. B* **2005**, 109, 21858–21864.
- (23) Marinova, K. G.; Alargova, R. G.; Denkov, N. D.; Velev, O. D.; Petsev, D. N.; Ivanov, I. B.; Borwankar, R. P. Charging of oil-water interfaces due to spontaneous adsorption of hydroxyl ions. *Langmuir* 1996, 12, 2045–2051.
- (24) Roke, S.; Gonella, G. Nonlinear light scattering and spectroscopy of particles and droplets in liquids. *Annu. Rev. Phys. Chem.* **2012**, *63*, 353–378.
- (25) Scheu, R.; Chen, Y.; de Aguiar, H. B.; Rankin, B. M.; Ben-Amotz, D.; Roke, S. Specific ion effects in amphiphile hydration and interface stabilization. *J. Am. Chem. Soc.* **2014**, *136*, 2040–2047.
- (26) Pullanchery, S.; Kulik, S.; Schönfeldová, T.; Cassone, G.; Hassanali, A.; Roke, S. pH drives electron density fluctuations that enhance electric field-induced liquid flow. *ChemRxiv* **2023**, DOI: 10.26434/chemrxiv-2023-mx4m7.
- (27) Uematsu, Y. Electrification of water interface. J. Phys.: Condens. Matter 2021, 33, 423001.
- (28) Fumagalli, L.; Esfandiar, A.; Fabregas, R.; Hu, S.; Ares, P.; Janardanan, A.; Yang, Q.; Radha, B.; Taniguchi, T.; Watanabe, K.; et al. Anomalously low dielectric constant of confined water. *Science* **2018**, 360, 1339–1342.
- (29) Matyushov, D. V. Dielectric susceptibility of water in the interface. J. Phys. Chem. B 2021, 125, 8282-8293.
- (30) Feynman, R. P.; Leighton, R. B.; Sands, M. The Feynman Lectures on Physics, Vol. II: Mainly Electromagnetism and Matter; Addison-Wesley: Reading, MA, 1964.
- (31) Dinpajooh, M.; Matyushov, D. V. Dielectric constant of water in the interface. *J. Chem. Phys.* **2016**, *145*, 014504.
- (32) Mondal, S.; Bagchi, B. Water layer at hydrophobic surface: Electrically dead but dynamically alive? *Nano Lett.* **2020**, *20*, 8959–8964.

- (33) Motevaselian, M. H.; Aluru, N. R. Universal reduction in dielectric response of confined fluids. *ACS Nano* **2020**, *14*, 12761–12770.
- (34) Teschke, O.; Ceotto, G.; De Souza, E. F. Interfacial aqueous solutions dielectric constant measurements using atomic force microscopy. *Chem. Phys. Lett.* **2000**, 326, 328–334.
- (35) Debye, P.; Pauling, L. The inter-ionic attraction theory of ionized solutes. IV. The influence of variation of dielectric constant on the limiting law for small concentrations. *J. Am. Chem. Soc.* **1925**, *47*, 2129–2134
- (36) Levine, S.; Mingins, J.; Bell, G. M. The discrete-ion effect in ionic double-layer theory. *J. Electroanal. Chem.* **1967**, *13*, 280–329.
- (37) Olivieri, J.-F.; Hynes, J. T.; Laage, D. Confined water's dielectric constant reduction is due to the surrounding low dielectric media and not to interfacial molecular ordering. *J. Phys. Chem. Lett.* **2021**, *12*, 4319–4326.
- (38) Borgis, D.; Laage, D.; Belloni, L.; Jeanmairet, G. Dielectric response of confined water films: Insights from classical DFT. *ChemRxiv* 2023, arXiv:2302.03304.
- (39) Böttcher, C. J. F. Theory of Electric Polarization, Vol. 1: Dielectrics in Static Fields; Elsevier: Amsterdam, 1973.
- (40) Dinpajooh, M.; Matyushov, D. V. Free energy of ion hydration: Interface susceptibility and scaling with the ion size. *J. Chem. Phys.* **2015**, *143*, 044511.
- (41) Dufils, T.; Schran, C.; Chen, J.; Geim, A. K.; Fumagalli, L.; Michaelides, A. Origin of dielectric polarization suppression in confined water from first principles. *Chem. Sci.* **2024**, *15*, 516–527.
- (42) Ben-Amotz, D. Unveiling Electron Promiscuity. J. Phys. Chem. Lett. 2011, 2, 1216–1222.
- (43) Gonella, G.; Backus, E. H. G.; Nagata, Y.; Bonthuis, D. J.; Loche, P.; Schlaich, A.; Netz, R. R.; Kühnle, A.; McCrum, I. T.; Koper, M. T. M.; et al. Water at charged interfaces. *Nat. Rev. Chem* **2021**, *5*, 466–485.
- (44) Xiong, H.; Lee, J. K.; Zare, R. N.; Min, W. Strong electric field observed at the interface of aqueous microdroplets. *J. Phys. Chem. Lett.* **2020**, *11*, 7423–7428.
- (45) Remsing, R. C.; Baer, M. D.; Schenter, G. K.; Mundy, C. J.; Weeks, J. D. The Role of Broken Symmetry in Solvation of a Spherical Cavity in Classical and Quantum Water Models. *J. Phys. Chem. Lett.* **2014**, *5*, 2767–2774.
- (46) Beattie, J. K.; Djerdjev, A. M. The pristine oil/water interface: Surfactant-free hydroxide-charged emulsions. *Angew. Chem., Int. Ed.* **2004**, *43*, 3568–3571.
- (47) Carpenter, A. P.; Tran, E.; Altman, R. M.; Richmond, G. L. Formation and surface-stabilizing contributions to bare nanoemulsions created with negligible surface charge. *Proc. Natl. Acad. Sci. U.S.A.* **2019**, *116*, 9214–9219.
- (48) Samanta, T.; Matyushov, D. V. Ionic mobility driven by correlated van der Waals and electrostatic forces. *J. Chem. Phys.* **2022**, *156*, 204501.
- (49) Sarhangi, S. M.; Waskasi, M. M.; Hashemianzadeh, S. M.; Matyushov, D. V. Effective dielectric constant of water at the interface with charged  $C_{60}$  fullerenes. *J. Phys. Chem. B* **2019**, *123*, 3135–3143.
- (50) Sundararaman, R.; Schwarz, K. Solvent effects determine the sign of the charges of maximum entropy and capacitance at silver electrodes. *J. Chem. Phys.* **2023**, *158*, 121102.
- (51) Lynden-Bell, R. M.; Rasaiah, J. C. From hydrophobic to hydrophilic behaviour: A simulation study of solvation entropy and free energy of simple solutes. *J. Chem. Phys.* **1997**, *107*, 1981–1991.
- (52) Hummer, G.; Pratt, L. R.; Garcia, A. E. Molecular theories and simulation of ions and polar molecules in water. *J. Phys. Chem. A* **1998**, *102*, 7885–7895.
- (53) Mobley, D. L.; Barber, A. E.; Fennell, C. J.; Dill, K. A. Charge asymmetries in hydration of polar solutes. *J. Phys. Chem. B* **2008**, *112*, 2405–2414.
- (54) Carnie, S. L.; Patey, G. N. Fluids of polarizable hard spheres with dipoles and tetrahedral quadrupoles. Integral equation results with application to liquid water. *Mol. Phys.* **1982**, *47*, 1129–1151.

- (55) Davis, J. G.; Gierszal, K. P.; Wang, P.; Ben-Amotz, D. Water structural transformation at molecular hydrophobic interfaces. *Nature* **2012**, *491*, 582–585.
- (56) Shandilya, A.; Schwarz, K.; Sundararaman, R. Interfacial water asymmetry at ideal electrochemical interfaces. *J. Chem. Phys.* **2022**, *156*, 014705.
- (57) Liu, W.-T.; Shen, Y. R. In situ sum-frequency vibrational spectroscopy of electrochemical interfaces with surface plasmon resonance. *Proc. Natl. Acad. Sci. U.S.A.* **2014**, *111*, 1293–1297.
- (58) Velasco-Velez, J.-J.; Wu, C. H.; Pascal, T. A.; Wan, L. F.; Guo, J.; Prendergast, D.; Salmeron, M. The structure of interfacial water on gold electrodes studied by x-ray absorption spectroscopy. *Science* **2014**, *346*, 831–834
- (59) Wang, Y.-H.; Zheng, S.; Yang, W.-M.; Zhou, R.-Y.; He, Q.-F.; Radjenovic, P.; Dong, J.-C.; Li, S.; Zheng, J.; Yang, Z.-L.; et al. In situ Raman spectroscopy reveals the structure and dissociation of interfacial water. *Nature* **2021**, *600*, 81–85.
- (60) Li, C.-Y.; Le, J.-B.; Wang, Y.-H.; Chen, S.; Yang, Z.-L.; Li, J.-F.; Cheng, J.; Tian, Z.-Q. In situ probing electrified interfacial water structures at atomically flat surfaces. *Nat. Mater.* **2019**, *18*, 697–701.
- (61) Montenegro, A.; Dutta, C.; Mammetkuliev, M.; Shi, H.; Hou, B.; Bhattacharyya, D.; Zhao, B.; Cronin, S. B.; Benderskii, A. V. Asymmetric response of interfacial water to applied electric fields. *Nature* **2021**, *594*, 62–65.
- (62) Lotti, D.; Hamm, P.; Kraack, J. P. Surface-sensitive spectroelectrochemistry using ultrafast 2D ATR IR spectroscopy. *J. Phys. Chem.* C 2016, 120, 2883–2892.
- (63) Ryan, M. J.; Yang, N.; Kwac, K.; Wilhelm, K. B.; Chi, B. K.; Weix, D. J.; Cho, M.; Zanni, M. T. The hydrogen-bonding dynamics of water to a nitrile-functionalized electrode is modulated by voltage according to ultrafast 2D IR spectroscopy. *Proc. Natl. Acad. Sci. U.S.A.* **2023**, *120*, No. e2314998120.
- (64) Wang, Y.; Seki, T.; Yu, X.; Yu, C.-C.; Chiang, K.-Y.; Domke, K. F.; Hunger, J.; Chen, Y.; Nagata, Y.; Bonn, M. Chemistry governs water organization at a graphene electrode. *Nature* **2023**, *615*, E1–E2.
- (65) Richert, R. Supercooled liquids and glasses by dielectric relaxation spectroscopy. *Adv. Chem. Phys.* **2014**, *156*, 101–195.
- (66) Pajkossy, T.; Kolb, D. M. Double layer capacitance of Pt(111) single crystal electrodes. *Electrochim. Acta* **2001**, *46*, 3063–3071.
- (67) Stratton, J. A. Electromagnetic Theory; McGraw-Hill Inc.: New York, 1941.
- (68) Matyushov, D. V. Manual for Theoretical Chemistry; World Scientific Publishing Co. Pte. Ltd.: New Jersey, 2021.
- (69) Samanta, T.; Sarhangi, S. M.; Matyushov, D. V. Enhanced Molecular Diffusivity through Destructive Interference between Electrostatic and Osmotic Forces. *J. Phys. Chem. Lett.* **2021**, *12*, 6648–6653.
- (70) Matyushov, D. V. Electrophoretic mobility without charge driven by polarisation of the nanoparticle—water interface. *Mol. Phys.* **2014**, *112*, 2029—2039.
- (71) Martin, D. R.; Friesen, A. D.; Matyushov, D. V. Electric field inside a "Rossky cavity" in uniformly polarized water. *J. Chem. Phys.* **2011**, *135*, 084514.
- (72) Pethig, R. Dielectrophoresis. Theory, Methodology and Biological Applications; Wiley: Hoboken, NJ, 2017.
- (73) Uematsu, Y.; Bonthuis, D. J.; Netz, R. R. Nanomolar surface-active charged impurities account for the zeta potential of hydrophobic surfaces. *Langmuir* **2020**, *36*, 3645–3658.
- (74) Pel, J.; Broemeling, D.; Mai, L.; Poon, H.-L.; Tropini, G.; Warren, R.; Holt, R. A.; Marziali, A. Nonlinear electrophoretic response yields a unique parameter for separation of biomolecules. *Proc. Natl. Acad. Sci. U.S.A.* **2009**, *106*, 14796–14801.
- (75) Lamontagne, M.; Levy, S. Nonlinear electrophoretic velocity of DNA in slitlike confinement. *Phys. Rev. E* **2022**, *105*, 054503.
- (76) Roger, K.; Cabane, B. Why are hydrophobic/water interfaces negatively charged? *Angew. Chem., Int. Ed.* **2012**, *51*, 5625–5628.
- (77) Stachurski, J.; MichaŁek, M. The effect of the  $\zeta$  potential on the stability of a non-polar oil-in-water emulsion. *J. Colloid Interface Sci.* **1996**, 184, 433–436.

ı

- (78) O'Brien, R. W.; Beattie, J. K.; Djerdjev, A. M. The electrophoretic mobility of an uncharged particle. *J. Colloid Interface Sci.* **2014**, 420, 70–73.
- (79) Vácha, R.; Horinek, D.; Berkowitz, M. L.; Jungwirth, P. Hydronium and hydroxide at the interface between water and hydrophobic media. *Phys. Chem. Chem. Phys.* **2008**, *10*, 4975–4980.
- (80) Petersen, P. B.; Saykally, R. J. Is the liquid water surface basic or acidic? Macroscopic vs. molecular-scale investigations. *Chem. Phys. Lett.* **2008**, 458, 255–261.
- (81) Samson, J.-S.; Scheu, R.; Smolentsev, N.; Rick, S. W.; Roke, S. Sum frequency spectroscopy of the hydrophobic nanodroplet/water interface: Absence of hydroxyl ion and dangling OH bond signatures. *Chem. Phys. Lett.* **2014**, *615*, 124–131.
- (82) Sanders, S. E.; Vanselous, H.; Petersen, P. B. Water at surfaces with tunable surface chemistries. *J. Phys.: Condens.Matter* **2018**, *30*, 113001–113026.
- (83) Dinpajooh, M.; Matyushov, D. V. Mobility of nanometer-size solutes in water driven by electric field. *Phys. A* **2016**, 463, 366–375. (84) Hummer, G.; Garde, S. Cavity Expulsion and Weak Dewetting of Hydrophobic Solutes in Water. *Phys. Rev. Lett.* **1998**, 80, 4193–4196.